

Undergraduate Laboratory Experiment

TEACHING FUNDAMENTAL CONCEPTS OF MAGNETIC MATERIALS IN THE CONTEXT OF NANOPARTICLE HYPERTHERMIA FOR CANCER TREATMENT

TYLER COOPER¹, RUSSELL TRAFFORD², ANILCHANDRA ATTALURI³, AND ANDREA JENNIFER VERNENGO¹

1 Department of Chemical Engineering, Rowan University, Glassboro, NJ

2 Department of Electrical and Computer Engineering, Rowan University, Glassboro, NJ

3 Department of Mechanical Engineering, The Pennsylvania State University – Harrisburg, PA

Hyperthermia is a relatively new approach to treating various types of cancers. It involves heating the cancerous tissues in order to induce cell death. Conventionally, hyperthermia is achieved by ultrasound, microwaves, or infrared radiation, but these approaches are likely to heat the surrounding healthy tissues, causing damage.^[1,2] More recently, selective heating of tumors has been achieved by the application of magnetic nanoparticles to the tumor site, which will generate heat when exposed to alternating magnetic fields (AMF).^[3,4] The heat output, typically quantified by the specific loss power (SLP), depends on the AMF frequency and amplitude, as well as the chemical and physical properties of the nanoparticles.^[5] Optimization of the magnetic nanoparticle hyperthermia requires the application of concepts across multiple disciplines, including chemistry, electrical engineering, physics, and materials science. Therefore, this technology presents an opportunity to teach students foundational concepts in science and engineering. In the following experiment, students use an AMF coil attached to an induction power supply to study the temperature vs. time behavior of magnetic nanoparticles under varying conditions. The learning objectives of this laboratory module are:

- *To explain the general properties of magnetic materials and magnetic nanoparticles.*
- *To describe the application of magnetic nanoparticle hyperthermia to cancer therapy.*

- *To describe the mechanisms of heating of single- and multiple-domain magnetic materials.*
- *To quantify the effect of applied current, suspension viscosity, and nanoparticle concentration on the SLP and explain the phenomenon within the context of Brownian and Néel relaxation time.*

Andrea Vernengo is an associate professor of chemical and biomedical Engineering (joint appointment) and director of the Tissue Engineering and Biomaterials Laboratory of the Henry M. Rowan College of Engineering. Andrea received her Ph.D. from Drexel University in 2007. She has 15 years of research experience in the development of novel biomaterials for repair and regeneration of the intervertebral disc. Additionally, through an NSF TUES grant, she has developed novel hands-on laboratory activities that use biomaterials science and tissue engineering to teach undergraduates core STEM principles.

Anilchandra Attaluri is an assistant professor of mechanical engineering in the School of Science, Engineering, and Technology of Penn State Harrisburg. He received his Ph.D. from the University of Maryland Department of Mechanical Engineering in 2012. Following completion of his Ph.D., Anilchandra joined the Department of Radiation Oncology & Molecular Radiation Sciences at Johns Hopkins University School of Medicine as a post-doctoral research fellow. Currently, he is focused on developing novel devices and treatment planning systems for cancer treatments.

Russell Trafford obtained his B.S. in electrical and computer engineering from Rowan University in 2016. Currently, he is at Rowan University pursuing his doctoral degree in electrical and computer engineering.

Tyler Cooper obtained his B.S. in chemical engineering from Rowan University in 2016. Currently, Tyler Cooper is the laboratory manager in the Technical Operations department at Amicus Therapeutics.

The laboratory was implemented into a junior-level materials science course at Rowan University. During the first semester offering, the lab was implemented into an online version of the course, so the students received raw data in electronic form. In the subsequent course offering, it was run as a hybrid, so the students synthesized their own nanoparticles and did the heating study in a face-to-face session. Both cohorts then proceeded with the same data analysis. Outcomes for the two formats were compared with student surveys and pre- and post tests.

LITERATURE REVIEW

Hyperthermia in Cancer Treatment

The idea of using localized temperature to destroy cells is called hyperthermia. When cancer cells are heated to temperatures between 42-46°C, the result is cellular inactivation.^[6] One approach to achieve hyperthermia is to embed nanometer-sized magnetic particles dispersed in a liquid medium into a tumor. In the presence of AMF frequencies below 300 KHz,^[7] selective heating of the nanoparticles will occur.^[1,4] Magnetite (Fe₃O₄) nanoparticles have been widely studied for hyperthermia applications due to their strong magnetic properties and low toxicity.^[8] Shown in Figure 1 is a temperature vs. time curve for a 5 mg/mL aqueous suspension of magnetite nanoparticles (Micromod, GmBH, Rostock, Germany) heated with AMF using an Ambrell EasyHeat 0112 induction heater attached to a three-turn copper coil and an applied frequency of 280 KHz.

Magnetite Nanoparticles

Various methods of chemical synthesis are known for the production of magnetite nanoparticles. One route is the coprecipitation of ferric chloride (FeCl₃) and ferrous sulfate heptahydrate (FeSO₄ · 7H₂O) at basic pH, as described by Rashad, et al.^[9] The size of the nanoparticles produced with this method was shown to range from 9-12 nm.

Due to van der Waals forces and magnetic dipole interactions between particles, magnetite tends to agglomerate when suspended in aqueous medium.^[10] It has been shown that coating the nanoparticles with a hydrophilic polymer such as chitosan or starch^[11,12] prevents the formation of large aggregates and enhances the hyperthermic effect.^[13] In hyperthermia studies, the specific loss power [SLP, Eq. (1)] is a measure of the heat generated by magnetic particles in an AMF.^[14]

$$SLP = \frac{C}{m_{\text{magnetic}}} \cdot \frac{dT}{dt} \quad (1)$$

In Eq. (1), C is the sample-specific heat capacity, m_{magnetic} is the mass of nanoparticles per total mass of suspension, and $\frac{dT}{dt}$ is the slope of the time dependent temperature curve for adiabatic systems. To our knowledge there is only one adiabatic magneto-thermal calorimetric system.^[15] Most laboratories

use quasi-adiabatic systems by surrounding a test tube, which contains magnetic fluid, with a thermal insulator such as Styrofoam®. Use of Eq. (1) involves three thermodynamic assumptions^[16,17]: (i) sample is at thermal equilibrium before turning on the AMF, (ii) internal thermal mixing in the sample happens within a short time duration (< 1 s or time constant of the temperature probe), and (iii) $\frac{dT}{dt}$ should be calculated using the time range before the start of heat loss from the sample to the surrounding (only the first 60 seconds of heating was considered in this study). The heat capacity of the sample can be taken as that of water if the nanoparticles are present in low concentrations (below 5 mg/mL). Otherwise, the heat capacity of the sample can be calculated as the mass weighted mean value of the nanoparticles and water.^[18]

Diamagnetism and Paramagnetism

Basic concepts of magnetism help explain why magnetic nanoparticles heat in the presence of AMF. All atoms have a magnetic moment associated with them, which comes from orbital motion of electrons around the nucleus, as well as each electron spinning around on an axis. In diamagnetic materials, an external magnetic field will exert a torque on the electrons, changing the orbital motion such that it will be oriented in a direction opposite to the field, creating a net dipole moment. In paramagnetic materials, dipole moments preferentially align with the magnetic field. Both paramagnetic and diamagnetic materials are considered nonmagnetic because, in the absence of a magnetic field, there is no net alignment of the magnetic moments.^[19]

Ferromagnetism and Ferrimagnetism

Ferromagnetism is a very common form of magnetism that occurs in certain transition metals, such as BCC α-ferrite.

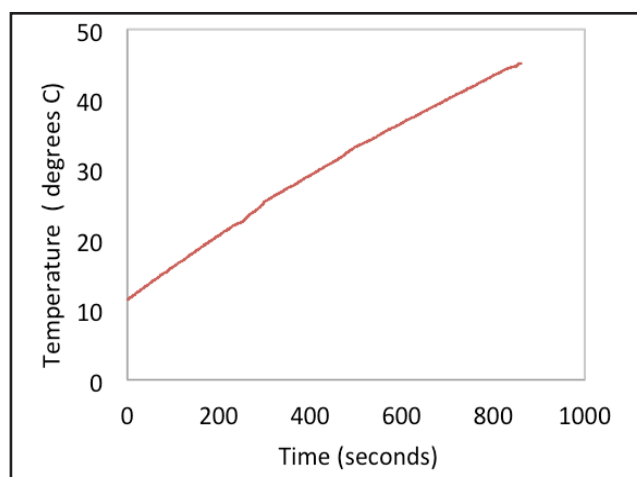


Figure 1. Temperature vs. time curve for a 5 mg/mL aqueous suspension of magnetite nanoparticles (Micromod) heated with an Ambrell EasyHeat 0112 attached to a three-turn copper coil and an applied frequency of 280 KHz.

Unlike in diamagnetic and paramagnetic materials, there exist large-volume regions, called domains, in which interactions between adjacent atoms cause the magnetic moments to align with each other, even in the absence of a magnetic field. Thus, there exist permanent magnetic moments within each domain. When an external magnetic field is applied, the magnetic moments in all of the domains may mutually align with the field. When this occurs, the magnetization reaches a saturation value, M_s .^[19]

Magnetite, Fe_3O_4 , is ferrimagnetic, which is similar to being ferromagnetic, except the material contains two different types of atoms with opposing moments. The Fe ions exist in both +2 and +3 states in a ratio of 1:2. Although the Fe^{3+} magnetic moments are opposite in direction, canceling each other out, the material is considered magnetic because the Fe^{2+} ions tend to align their moments even in the absence of an externally applied field.^[19]

AMF GENERATOR

There are many ways to generate an AMF. One way is to send a current, I , through a coil like the one shown in Figure 2A. If an object is placed within the coil, it would be exposed to an AMF amplitude, H , at constant frequency. The analytical expression used to estimate H at the center was obtained by assuming multiple loops with equal current and diameter.

$$H = \frac{N \cdot r^2}{\left(\left(\frac{d}{2}\right)^2 + r^2\right)^{3/2}} \cdot \frac{1}{2} \quad (2)$$

In Eq. (2), r is the average radius of the coil, d is the distance between the loops, and N is the number of turns stacked. Retrospectively, H of the manufactured three-turn water-cooled solenoid coil (Figure 2B) at different current settings was measured with a commercial 2-D magnetic field probe (AMF Lifesystems, Inc.) using the procedures described elsewhere.^[20] A calibration curve of H (kA/m) vs. current, I (A) was developed. From the calibration curve, current was proportional to the H (kA/m). Hence, different currents were used in the study to simplify the electromagnetic concepts for the target audience.

Behavior of Ferro- and Ferrimagnetic Materials in AMF

Consider a magnetic material in the presence of this magnetic field. The magnetic flux density, denoted B , represents the magnitude of the internal field strength within a substance subjected to an external magnetic field, H .

Any ferrimagnetic or ferromagnetic material, such as magnetite, is composed of regions where magnetic dipoles are aligned in the absence of a magnetic field. Each region, having a different magnetization orientation, is separated by a domain boundary. Thus, these are known as multiple domain materials. Consider the scenario where the material is subjected to an AMF. Prior to the application of the magnetic field, the domains in the material are randomly oriented such that there is no net B . However, as H is applied, the domains change shape and size as more and more dipole moments become aligned with the applied field. As the magnitude of the magnetic field increases, the flux density in the material will gradually increase^[19] as shown in Figure 3. Eventually, the macroscopic material will consist of a single domain and saturation magnetization (M_s) is reached, which is represented by the plateau in the curve in Figure 3.^[19]

Upon reversal of the magnetic field, portions of the material will have dipoles that become aligned with the new direction. During the reversal, the B field will decrease at a slower rate than the applied H field, an effect called hysteresis. When the H field reaches zero, there will still be a residual field B within the material, called the remanence. Remanence and hysteresis occur because there is resistance to moving of domain walls in response to the magnetic field switching direction. The shifting of domain walls in this way produces heat in the material and the

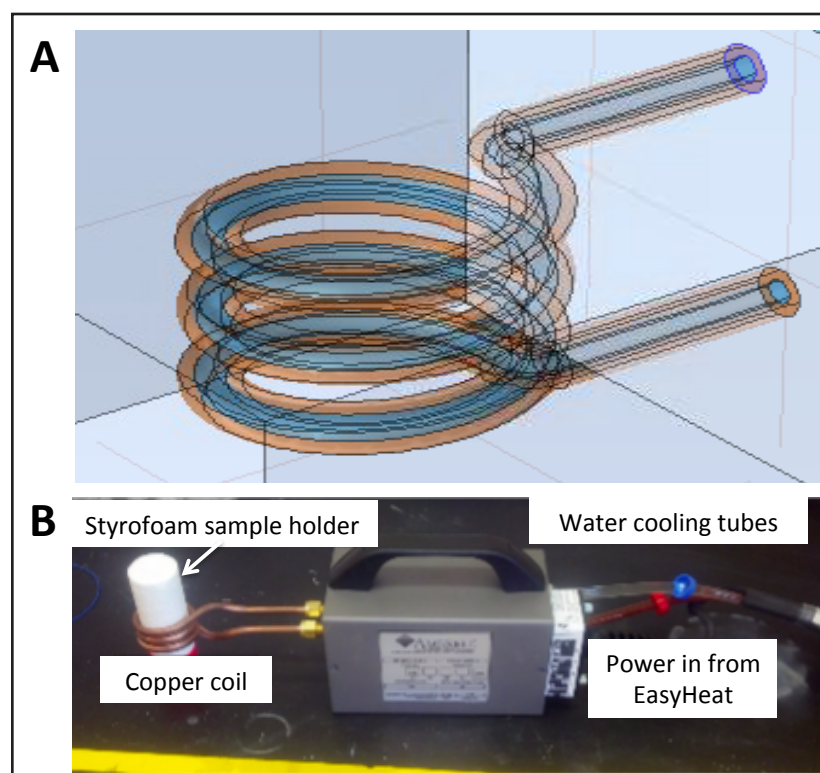


Figure 2. A three-turn water-cooled solenoid to generate AMF (A). A sample is placed within styrofoam casing in the center of the coil, which is attached to a work head connected to the EasyHeat power supply. Water runs through the coils for cooling during operation (B).

This activity, as it is designed, offers flexibility in the required time for completion of the face-to-face version.

resistance accounts for the lag in B .^[19] The anisotropy energy density, K , is the energy required to completely reverse the direction of the magnetization of the material.^[21]

Magnetization Behavior of Single-Domain Materials in AMF

As magnetite particle size decreases below a critical size of 50 nm,^[22] the material will consist of one domain rather than multiple domains. In a single domain material, all magnetic moments are aligned, even in the absence of a magnetic field. Thus, in the absence of domain walls, there is zero remanence, meaning that after removal of the magnetic field, the internal moment in the particles reduces to zero. However, single-domain materials do undergo hysteresis and exhibit heating in external magnetic fields, but the mechanism leading to this is different than multiple domain materials. The prevailing notion that the single domain particles are superparamagnetic is inconsistent with the literature. Some single domain particles might exhibit superparamagnetic behavior. Superparamagnetic particles do not generate heat—this would be a violation of second law of thermodynamics. A detailed explanation from the first law of thermodynamics is discussed in the recent seminal review paper.^[23] Hysteresis, in the case of single domain particles, arises because of the simultaneous rotation of the magnetic moments in the sample. According to simplified linear response theory, the magnetic moment rotates due to the torque exerted by the magnetic field, while the particle itself remains fixed, a process called Néel relaxation. When the anisotropy energy density of the sample is high compared to the external magnetic field, reversal of the magnetic moment is inhibited, which results in hysteresis. Like in multiple-domain particles, thermal energy is dissipated by the hysteresis. The rotation of the magnetic moment may also result in the rotation of the whole particle itself. Here, thermal energy is delivered through shear stress with the surrounding fluid, called Brownian relaxation. In suspensions of magnetic nanoparticles that are 50 nm or less, both mechanisms occur at the same time and the time scales at which they happen determine the relative contributions of each mechanism.^[24]

Néel relaxation has a time constant associated with it, τ_N , calculated with Eq. (3).^[25] The quantity τ_N essentially describes the time it takes for the magnetization to flip or reverse direction.

$$\tau_N = \frac{\tau_o}{2} \sqrt{\frac{nkT}{KV}} e^{KV/kT} \quad (3)$$

In Eq. (3), K is a temperature-dependent anisotropy energy

density,^[21] V is the volume of the particle, k is the Boltzmann constant, T is temperature, and τ_o is a constant characteristic of the material.

The Brownian relaxation also has a time constant associated with it, τ_B , that describes the time it takes for rotation of the whole particle. It can be calculated with Eq. (4).^[26]

$$\tau_B = \frac{3\eta V_H}{kT} \quad (4)$$

where η is the fluid viscosity and V_H is the hydrodynamic volume of the particle in the suspended liquid. When single domain particles are exposed to AMF, Brownian and Néel relaxation occur in parallel, so the system will have an effective relaxation time, τ , described by Eq. (5).^[26]

$$\frac{1}{\tau} = \frac{1}{\tau_B} + \frac{1}{\tau_N} \quad (5)$$

According to this equation, when τ_B is very large, then τ_N dominates the system and Néel relaxation is the principle cause of the heating. Factors that make τ_B very large are increased viscosity of the fluid medium in which the particles are suspended, increased particle size, and increased particle aggregation, all of which inhibit whole particle rotation.^[4]

PEDAGOGICAL FRAMEWORK

As nanotechnology research and development continues to progress and influence multiple sectors of the economy, more universities are beginning to offer courses and degree programs in the area. Some educational activities have been developed and assessed in topic areas loosely related to this lab activity. For instance, in one reported module, students synthesize their own gold and silver nanoparticles and assess the toxicology *in vitro*.^[27] In a module developed at the University of

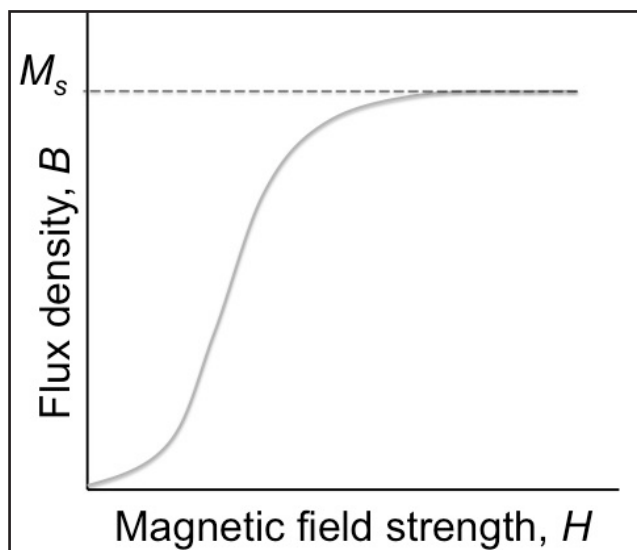


Figure 3. B vs. H behavior for a macroscopic ferro- or ferrimagnetic material. Adapted from Reference 19.

Cincinnati,^[28] students build an electromagnetic solenoid of copper wire to learn concepts in electromagnetics. Importantly, a recent study reported that concrete experiences with the physical phenomenon of magnetism are necessary to clear up conceptual misunderstandings among students, since it is a nonintuitive physical phenomenon.^[29]

LABORATORY DESCRIPTION

Overview

The aim of this experiment is to synthesize magnetic Fe_3O_4 nanoparticles and investigate the effect of three variables (applied current level, suspension viscosity, and nanoparticle concentration) on the heating capability of the nanoparticles. Temperature vs. time data is collected for three sets of samples, summarized in Table 1. In the first set (samples 1-12), current is applied at three different levels (175, 225, and 275 amps) to 100 mg/mL aqueous suspensions of Fe_3O_4 nanoparticles. In the next set (samples 13-18), the viscosity of the suspension is varied by adding 0, 20, or 60 vol% glycerol while the current is held constant at 275 amps and nanoparticle concentration at 100 mg/mL. In the last set (samples 19-21), the nanoparticle concentration in water is varied at 5 mg/mL or 100 mg/mL while the current is held constant at 275 amps. By comparing the SLP values for each set of data, students will apply what they learned about the heating mechanisms of single-domain particles to understanding how to control the heating rate.

Equipment

- Induction heating power supply (Ambrell EasyHeat 0112, equipped with a 0.66 μF capacitor, resonant frequency of 280 kHz)
- Three-turn water cooled copper coil (0.12m long)
- Multichannel temperature logger
- Optical temperature sensor
- Benchtop centrifuge

Materials

- Anhydrous ferric chloride
- Ferrous sulfate
- 5M sodium hydroxide
- Starch
- 5 mL polystyrene round bottom tubes with caps

Preparation of Fe_3O_4 Magnetic Nanoparticles

Fe_3O_4 particles are synthesized via a co-precipitation method, which is adapted from Rashad, et al.^[9]

1. Combine anhydrous ferric chloride and ferrous sulfate in a molar ratio of 2:1 for $\text{Fe}^{3+}:\text{Fe}^{2+}$ in aqueous solution.
2. Add 0.7 g/mL starch and stir manually.

Sample #	Nanoparticle concentration (mg/mL)	Applied Current (Amps)	Liquid medium composition
1-3	100	175	100% water
4-6	100	225	100% water
7-9	100	250	100% water
10-12	100	275	100% water
13-15	100	275	80 vol% water, 20% glycerol
16-18	100	275	40 vol% water, 60% glycerol
19-21	5	275	Water

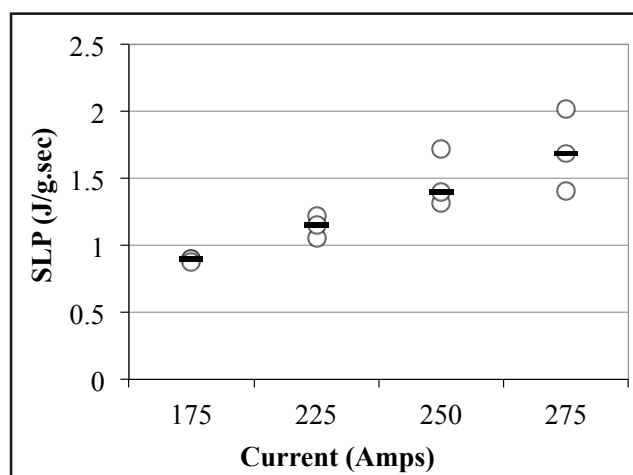


Figure 4. Scatterplot showing the relationship between SLP and applied current for 100 mg/mL Fe_3O_4 nanoparticles suspended in water and heated with AMF. The solid lines show the median difference.

3. Adjust the pH of the aqueous medium to 10 with the addition of 5 M sodium hydroxide while bubbling with inert gas.
4. Continue to bubble with inert gas for 30 minutes as the precipitation occurs.
5. Wash the product by repeated centrifugation at 2000 rpm for 3 minutes.
6. Suspend the particles at a concentration of 5 or 100 mg/mL in water or water/glycerol mixture with sonication for 20 minutes.
7. Transfer 1 mL aliquots of the particle suspensions into the round-bottom tubes for heating and store on ice until the start of testing.

Remote Heating of Magnetic Nanoparticles with AMF

1. Place the round-bottom tube containing the nanoparticle

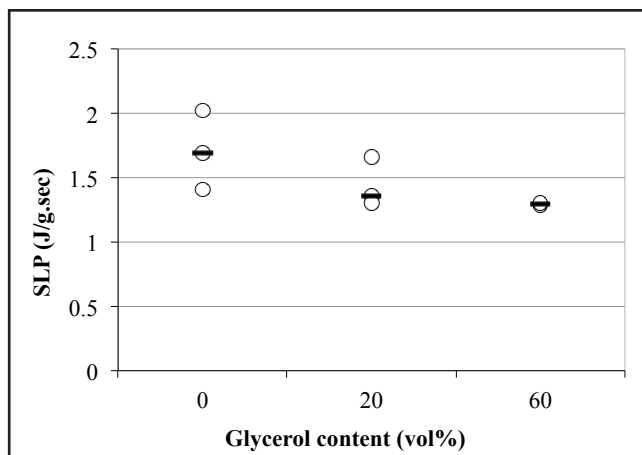


Figure 5. Scatterplot of SLP vs. glycerol content for suspensions of 100 mg/mL Fe_3O_4 nanoparticles. Current is held constant at 275 amps. The solid lines show the median difference.

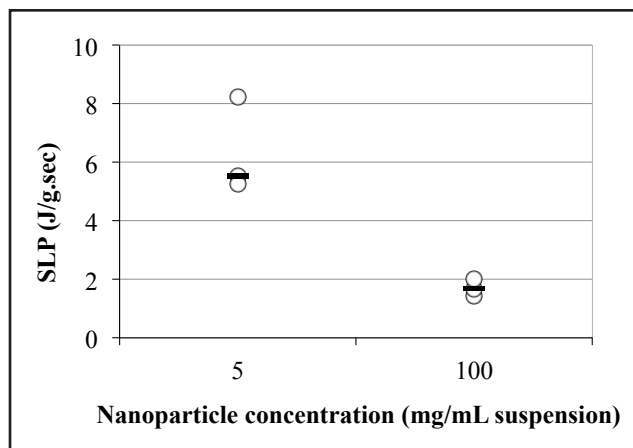


Figure 6. Scatterplot of SLP as nanoparticle concentration is varied from 5 to 100 mg/mL and current is held constant at 275 amps. The solid lines show the median difference.

suspensions in a styro-foam casing.

- Place the styrofoam + tube construct in the center of the coil (Figure 2B).
- The temperature is continuously monitored with an optical temperature sensor, placed into the suspension through a hole in the cap of the polystyrene tube. Temperature vs. time data is recorded every second with a Labview[®] interface and outputted to an Excel file.

DATA ANALYSIS

While students in the hybrid course performed the experiment in the above procedure in groups of four, those in the online course received raw temperature vs. time data in electronic form for samples 1-21 in Table 1. Both sections followed an identical guided data analysis to generate the graphs in Figures 6, 7, and 8. The SLP for each run was calculated with Eq. (1). Shown in Figure 4 is the relationship between average SLP and applied current for 100 mg/mL nanoparticles suspended in water. As current increases, the magnetic field strength increases, and this will enhance the extent of Brownian and Néel relaxation. This will also increase heat output of the nanoparticles, accounting for the increasing trend in SLP with current level.

Illustrated in Figure 5 is the average SLP vs. glycerol content for a constant current of 275 amps and nanoparticle concentration of 100 mg/mL. There is a small decreasing trend in SLP with increasing glycerol concentration. Glycerol

TABLE 2

Pre- and post test assessment questions were aligned to ABET Student Outcomes and Rowan outcomes for undergraduate chemical engineering students.

Outcome	Measurable skills categorized within this outcome
Student demonstrate an ability to apply knowledge of mathematics, science, and engineering (ABET - A)	Students will (1) explain the general properties of magnetic materials and magnetic nanoparticles; (2) describe the mechanisms of heating single- and multiple-domain magnetic materials.
Students demonstrate the ability to design and conduct experiments as well as to analyze and interpret data (ABET - B).	Students will analyze the effect of relevant experimental variables on the SLP and explain the phenomenon within the context of Brownian and Néel relaxation time.
Students demonstrate a knowledge of contemporary issues relevant to the field of chemical engineering (ABET - J).	Students demonstrate an awareness of how the principles of math, science, and engineering relevant to this laboratory activity are applicable to current medical technology.

increases the viscosity of the liquid suspension of nanoparticles. This will theoretically decrease the Brownian contribution to the heating,^[24] which could account for this trend.

Lastly, average SLP vs. nanoparticle concentration, using a constant current of 275 Amps, is shown in Figure 6. The SLP is significantly lower for higher concentrations of nanoparticles in aqueous suspension. A high concentration of nanoparticles likely causes large magnetite aggregates to form, which has been reported to limit Brownian relaxation.^[4,13,24] This causes the heat output per gram of particles per unit time to decrease.

SUMMARY OF ASSESSMENT AND LEARNING

To evaluate the impact of this experiment on student learning, a quiz was administered to students before and after the lab. The quiz was comprised of 14 multiple-choice questions, which were mapped to student outcomes set forth by ABET and the Rowan Chemical Engineering Department for its students. These outcomes, as well as measurable skills that are associated with each, are summarized in Table 2. A sample

of the quiz questions is provided in Table 3 in which the answers to the multiple-choice questions are presented as correct statements for brevity. (Full assessment quizzes, along with raw data files and lab handouts, are available for download at <bmelearninglab.com>. Users navigate to the “Units” tab and click on the “Magnetism” resource.) The average scores on the pre- and post tests were analyzed with a t-test using a 95% confidence interval ($\alpha = 0.05$).

Shown in Figure 7 are the average quiz scores for the hybrid and online sections. The average score on the pre-test combined for both sections ($n=46$ total) was $45 \pm 12\%$ ($p < 0.05$). Analyzed separately, the average score on the pre-test was $45 \pm 12\%$ for the online class and $43 \pm 11\%$ for the hybrid section. The post test score was $83 \pm 13\%$ for the online section

($n=26$) and $69 \pm 13\%$ for the hybrid section ($n=22$). Post test scores were significantly higher in both sections ($p < 0.05$), but the scores were not improved when the students completed the lab face-to-face. Between the pre-test and the post test, the percentage of correct responses increased by 26, 34, and 52% for ABET Student Outcomes a, b, and j, respectively, for the hybrid section (Figure 8). The online section also saw appreciable increases, at 31, 33, and 36% for ABET Student Outcomes a, b, and j, respectively (data not shown).

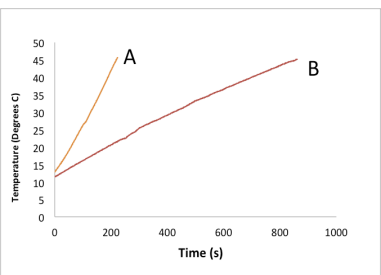
This activity, as it is designed, offers flexibility in the required time for completion of the face-to-face version. For instance, variables like suspension viscosity can be excluded. As an alternative, groups of students can study the different variables (current, suspension viscosity, or nanoparticle concentration) in parallel during a single laboratory period if multiple power supplies are available. The experiment, both in its online and face-to-face versions, can be expanded to encompass higher levels of complexity. For instance, the nanoparticles can be injected into agar gels and the temperature measured at various radial distances from the nanoparticles. Such an experiment would fit nicely into a heat transfer course. Experimental results could also be compared with modeling simulations.

In this work both study cohorts (online and hybrid) received the same lecture and laboratory handouts prior to the lab and were assessed with the same pre- and post test tool. Although the results did not indicate that the hands-on activity improved learning, there are other outcomes that were not captured with our assessment tool. Hands-on learners obtained practical experience with experimental methods, measurements, and experimental error that may help them tackle future real-life engineering problems.

CONCLUSIONS

Students use a solenoid coil attached to an induction power supply to study the temperature vs. time behavior of magnetic nanoparticles under varying current (AMF amplitude), suspension viscosity, and nanoparticle concentration. The laboratory was utilized in a junior-level materials science course at Rowan University. During the first semester offering, the lab was implemented into an online version of the course, so the students received raw data

TABLE 3
Sample of pre-and post test questions with answers presented as correct statements

Question	Correct Answer								
Which of the following most accurately describes the use of hyperthermia for cancer therapy?	The use of localized temperature between 42-46°C to destroy cells.								
Which of the following most accurately describes the phenomenon of hysteresis in ferri- and ferromagnetic materials?	When the B field within a magnetized material decreases at a lower rate than the applied field H due to resistance to motion of domain walls with the reversed field.								
When single domain particles are suspended in a highly viscous polymer, the mechanism that will likely dominate heating is:	Neel relaxation								
Which of the curves represents particles with a higher SLP? 	Curve A								
The following data was collected for three different nanoparticle suspensions. In each group, the same single domain nanoparticles, with average diameter of 9 nm, were used. Check all the statements that correctly apply: <table border="1" data-bbox="191 1766 467 1896"> <thead> <tr> <th>Group</th> <th>Average SLP</th> </tr> </thead> <tbody> <tr> <td>1</td> <td>8</td> </tr> <tr> <td>2</td> <td>12</td> </tr> <tr> <td>3</td> <td>16</td> </tr> </tbody> </table>	Group	Average SLP	1	8	2	12	3	16	i) Group 1 was possibly run at a lower applied current than Groups 2 and 3. ii) Group 1 was possibly run at a lower magnetic field strength compared to Group 2 and 3, iii) Group 1 exhibited a slower temperature rise than Groups 2 and 3.
Group	Average SLP								
1	8								
2	12								
3	16								

in electronic form. In the subsequent course offering, the course was offered as a hybrid, so the students synthesized their own nanoparticles and did the heating study hands-on before proceeding with the same data reduction and analysis. Outcomes were compared with pre- and post tests. Overall, the results indicated that the experiment contributed to student outcomes set forth by ABET for undergraduate engineering students. Average scores on the post test were not improved by having students perform the experiment hands-on. These results are promising because they may indicate that distance learning can be as effective as face-to-face classroom sessions.

ACKNOWLEDGMENT

This material is based upon work supported by the National Science Foundation under Grant No. 1245595.

REFERENCES

1. Verma J, Lal S, & Van Noorden CJF (2014) Nanoparticles for hyperthermic therapy: synthesis strategies and applications in glioblastoma. *Int. J. Nanomedicine* 9:2867-2877.
2. Jordan A (2006) *Hyperthermia in Cancer Treatment: A Primer*, G. Baronzio & Hager ED, Eds. (Springer: New York) p. 60-63.
3. Ito A, Shinkai M, Honda H, & Kobayashi T (2005) Medical application of functionalized magnetic nanoparticles. *J. Bioscience and Bioengineering* 100(1):1-11.
4. Deatsch AE & Evans BA (2014) Heating efficiency in magnetic nanoparticle hyperthermia. *J. Magnetism and Magnetic Materials* 354:163-172.
5. Gilchrist RK, Medal R, Shorey WD, Hanselman RC, Parrot JC & Taylor CB (1957) Selective inductive heating of lymph nodes. *Annals of Surgery* 146(4):596-606.
6. Streffer C & van Veuning D (1987) The biological basis for tumor therapy by hyperthermia and radiation, in *Hyperthermia and the Therapy of Malignant Tumors*, J Streffer, Ed. (Springer: Berlin) p. 24-70.
7. Kallumadil M, Tada T, Nakagawa M, Abe P, Souther P & Pankhurst QA (2009) Suitability of commercial colloids for magnetic hyperthermia. *J. Magnetism and Magnetic Materials* 321(10):1509-1513.
8. Shundo C, Zhang H, Nakanishi T & Osaka T (2012) Cytotoxicity evaluation of magnetite (Fe₃O₄) nanoparticles in mouse embryonic cells. *Colloids and Surfaces B: Biointerfaces* 97:221-225.
9. Rashad MM, El-Sayed HM, Rasly M & Nasr MI (2012) Induction heat-

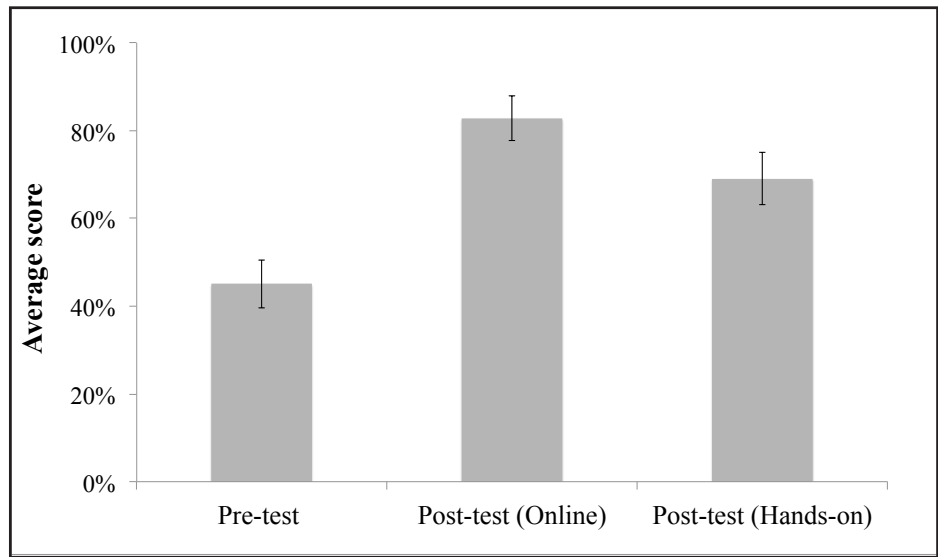


Figure 7. Average score on the pre-test ($n=46$ total) vs. post test for the online section ($n=26$) and hybrid course ($n=22$). Post test scores were significantly higher in both sections ($p < 0.05$). Error bars represent 95% confidence intervals.

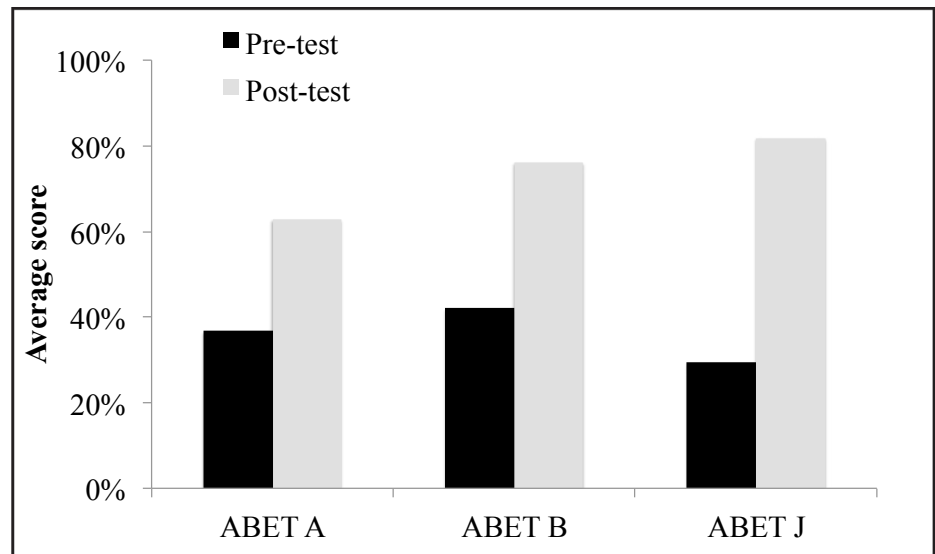


Figure 8. Percentage correct responses for each learning outcome listed in Table 2 for the hybrid course. The percent includes responses for questions mapped to a particular outcome.

- ing studies of magnetite nanospheres synthesized at room temperature for magnetic hyperthermia. *J. Magnetism and Magnetic Materials* 324: 4109-4023.
10. Jadhav NV, Prasad AI, Kumar A, Mishra R, Dhara S, Babu KR, Prajapat CL, Ningthoujam BN & Vatsa RK (2013) Synthesis of oleic acid functionalized Fe₃O₄ magnetic nanoparticles and studying their interaction with tumor cells for potential hyperthermia applications. *Colloids and Surfaces B: Biointerfaces* 108(1):158-168.
11. Kim DH, Lee SH, Im KH, Kim KN, Kim KM, Shim LB, Lee MH, Lee M & Lee Y-K (2006) Surface-modified magnetite nanoparticles for hyperthermia: Preparation, characterization, and cytotoxicity studies. *Current Applied Physics* 6S1:e242-e246.
12. Darroudi M, Hakimi M, Goodarzi E & Oskuee RK (2014) Super-

- paramagnetic iron oxide nanoparticles (SPIONs): Green preparation, characterization and their cytotoxicity effects. *Ceramics International* 40:14641-14645.
13. Erne BH, Butter K, Kuipers BWM & Vroege GJ (2003) Rotational diffusion in iron ferrofluids. *Langmuir* 19:8218.
 14. Lima E Jr, Torres TE, Rossi LM, Rechenberg HR, Berquo TS & Ibarra A (2013) Size dependence of the magnetic relaxation and specific power absorption in iron oxide nanoparticles. *J. Nanoparticle Research*, 15(5):1-11.
 15. Natividad E, Castro M & Mediano A (2009) Adiabatic vs. non-adiabatic determination of specific absorption rate of ferrofluids. *J. Magnetism and Magnetic Materials* 321(10):1497-1500.
 16. Bordelon D, et al. (2011) Magnetic nanoparticle heating efficiency reveals magneto-structural differences when characterized with wide ranging and high amplitude alternating magnetic fields. *J. Applied Physics* 109(12):124904.
 17. Attaluri A, et al. (2013) Calibration of a quasi-adiabatic magneto-thermal calorimeter used to characterize magnetic nanoparticle heating. *J Nanotechnology in Engineering and Medicine* 4(1):011006.
 18. Shete PB, Patil RM, Thorat ND, Prasad A, Ningthoujam RS, Ghosh SJ & Pawa SH (2014) Magnetic chitosan nanocomposite for hyperthermia therapy application: Preparation, characterization and in vitro experiments. *Applied Surface Science* 288:149-157.
 19. Callister WD & Rethwisch DG (2013) *Materials Science and Engineering* (Wiley).
 20. Attaluri A, Nusbaum C, Wabler W & Ivkov R (2013) Calibration of a quasi-adiabatic magneto-thermal calorimeter used to characterize magnetic nanoparticle heating. *J. Nanotechnology in Engineering and Medicine* 4(1):011006.
 21. Yoon S & Krishnan KM (2011) Temperature dependence of magnetic anisotropy constant in manganese ferrite nanoparticles at low temperature. *J. Applied Physics* 109:07B534.
 22. Dormann JL, Firoani D & Tronc E (1997) Magnetic relaxation in fine-particle systems, in *Advances in Chemical Physics*, Prigogine I & Rice SA, Eds. (Wiley: New York).
 23. Dennis C & Ivkov R (2013) Physics of heat generation using magnetic nanoparticles for hyperthermia. *Int. J. Hyperthermia* 29(8):715-729.
 24. Chen S, Chiang C & Hsieh S (2010) Simulating physiological conditions to evaluate nanoparticles for magnetic fluid hyperthermia (MFH) therapy applications. *J. Magnetism and Magnetic Materials* 322:247-252.
 25. Néel L (1949) Theorie du Trainage Magnetique des Ferromagnetiques en Grains Fins avec Applications aux Terres Cuites. *Annales Geophysicae* 5:99-136.
 26. Rosensweig RE (2002) Heating magnetic fluid with alternating magnetic field. *J. Magnetism and Magnetic Materials* 252:370-374.
 27. Pierce S, Lowery A, Bell C & Giorgio TAC (2010) Nanoparticle synthesis to application: A nanobiotechnology lab course for biomedical engineering. *Proceedings American Society for Engineering Education Annual Meeting and Exposition*.
 28. Boerio F, Dionysiou DD, Papautsky I, Pelaez M, Schulz M, Huth C & Shanov V. (2011) Nanotechnology in undergraduate education: Development of experiment modules. *Proceedings of the American Society for Engineering Education*.
 29. Singh C (2008) Improving students' understanding of magnetism, *Proceedings of the American Society for Engineering Education Annual Conference and Exposition*. □